Energetics of Cooperative Protein-DNA Interactions: Comparison between Quantitative Deoxyribonuclease Footprint Titration and Filter Binding†

Donald F. Senear, Michael Brenowitz, Madeline A. Shea, and Gary K. Ackers*

Department of Biology and McCollum-Pratt Institute, The Johns Hopkins University, Baltimore, Maryland 21218

Received May 12, 1986; Revised Manuscript Received June 27, 1986

ABSTRACT: Using the binding of *cI* repressor protein to the λ right and left operators as a model system, we have analyzed the two common experimental techniques for studying the interactions of genome regulatory proteins with multiple, specific sites on DNA. These are the quantitative DNase footprint titration technique [Brenowitz, M., Senear, D. F., Shea, M. A., & Ackers, G. K. (1986) *Methods Enzymol. 130*, 132-181] and the nitrocellulose filter binding assay [Riggs, A., Suzuki, H., & Bourgeois, S. (1970) *J. Mol. Biol. 48*, 67-83]. The footprint titration technique provides binding curves that separately represent the fractional saturation for each site. In principle, such data contain the information necessary to determine the thermodynamic constants for local site binding and cooperativity. We show that in practice, this is not possible for all values of the constants in multisite systems, such as the λ operators. We show how these constants can nevertheless be uniquely determined by using additional binding data from a small number of mutant operators in which the number of binding sites has been reduced. The filter binding technique does not distinguish binding to the individual sites and yields only macroscopic binding parameters which are composite averages of the various local site and cooperativity constants. Moreover, the resolution of even macroscopic constants from filter binding data for multisite systems requires ad hoc assumptions as to a relationship between the number of ligands bound and the filter retention of the complex. Our results indicate that no such relationship exists. Hence, the technique does not permit determination of thermodynamically valid interaction constants (even macroscopic) in multisite systems.

The regulation of genomic processes such as replication, recombination, repair, and transcription involves the interaction of protein ligands with DNA. Understanding the molecular mechanism of regulation requires a thermodynamic analysis of the interactions between the regulatory proteins and their specific DNA binding sites. Several methods have been developed to monitor the extremely high-affinity binding that is typically exhibited by DNA binding proteins. These include the gel electrophoresis method of Garner and Revzin (1981) and of Fried and Crothers (1981), the recently developed gel chromatographic technique of Frankel et al. (1985), and the fluorescence technique of Draper and Gold (1980). However, the most popular technique continues to be the filter binding assay of Riggs et al. (1970), which relies on the ability of bound protein ligands to induce the retention of double-stranded DNA by nitrocellulose filters.

Technical simplicity and broad applicability are tremendous advantages of the filter binding technique. An elegant treatment by Woodbury and von Hippel (1983) outlines experimental designs and analytical approaches to allow estimation of binding parameters. As a consequence of these developments, filter binding continues to be the method of choice in most studies of protein-DNA interactions and genomic regulation.

The techniques listed above have in common that they do not distinguish between interactions at the individual, specific sites on the DNA. Consequently, they provide insufficient information to resolve the intrinsic free energies of interaction [see Ackers et al. (1983)]. By contrast, a method fully capable of distinguishing interactions at the individual sites is that of quantitative deoxyribonuclease (DNase)[1] footprint titration (Brenowitz et al., 1986a,b), an extension of the method of DNase protection mapping (Galas & Schmitz, 1978; Johnson et al., 1979). We have developed this method to be a rigorous, quantitative technique, applicable to a variety of experimental conditions. The method yields complete binding isotherms that separately represent the fractional saturation at each site.

In this paper, we present a comparative study on the footprint titration and filter binding techniques for analyzing site-specific binding of protein ligands to multiple sites on DNA. We have used, as a model system, the binding of bacteriophage λ *cI* repressor to λ right and left operators. Each operator consists of three binding sites to which repressor dimers bind cooperatively (Johnson et al., 1979). The λ right operator (O_R) is an excellent model system for these comparative studies, because of the availability of mutant DNA sequences, in which the number of the binding sites has been reduced in various combinations (Maurer et al., 1980; Meyer et al., 1980). By properly combining binding data for the wild-type O_R and these "reduced valency" mutant operators, microscopic binding and cooperativity constants are, in principle, resolvable by using any of the binding techniques described.

Our results show how it is possible to use the information provided by the footprint titration technique to resolve intrinsic binding constants and cooperativity terms when proteins bind

† This work was supported by National Institutes of Health Grant GM24486.

[1] Abbreviations: DNase I, bovine pancreas deoxyribonuclease I (EC 3.1.21.1); bis(acrylamide), *N,N'*-methylenebis(acrylamide); TEMED, *N,N,N',N'*-tetramethylethylenediamine; BSA, bovine serum albumin; CT DNA, calf thymus DNA; Tris, tris(hydroxymethyl)aminomethane; NaDodSO$_4$, sodium dodecyl sulfate; EDTA, (ethylenedinitrilo)tetraacetic acid; Bistris, [bis(2-hydroxyethyl)amino]tris(hydroxymethyl)methane; BRL, Bethesda Research Labs; O_L and O_R, λ left and right operators, respectively; bp, base pair(s).

0006-2960/86/0425-7344$01.50/0

Table I: Microscopic Configurations and Associated Free Energies for the λ Operator–Repressor Systems, O_R^+ and O_L^+[a]

species (s)	operator configuration: site 1		site 2		site 3	free energy contributions	total free energy
1	O		O		O	ref state	ΔG_{S1} (=0)
2	R_2		O		O	ΔG_1	ΔG_{S2}
3	O		R_2		O	ΔG_2	ΔG_{S3}
4	O		O		R_2	ΔG_3	ΔG_{S4}
5	R_2	↔	R_2		O	$\Delta G_1 + \Delta G_2 + \Delta G_{12}$	ΔG_{S5}
6	R_2		O		R_2	$\Delta G_1 + \Delta G_3$	ΔG_{S6}
7	O		R_2	↔	R_2	$\Delta G_2 + \Delta G_3 + \Delta G_{23}$	ΔG_{S7}
8	R_2	↔	R_2		R_2	$\Delta G_1 + \Delta G_2 + \Delta G_3 + \Delta G_{12}$	ΔG_{S8}
9	R_2		R_2	↔	R_2	$\Delta G_1 + \Delta G_2 + \Delta G_3 + \Delta G_{23}$	ΔG_{S9}

[a] Individual operator sites are denoted by O if vacant or by R_2 if occupied by repressor dimers. Pairwise interactions between adjacent occupied sites are denoted by (↔). ΔG_1, ΔG_2, and ΔG_3 are the intrinsic free energies of binding to the various individual sites and are related to the corresponding microscopic equilibrium constants, k_i, by the standard relationship $\Delta G_i = -RT \ln k_i$. ΔG_s represents the total free energy for a given configuration, relative to the reference configuration (s = 1). ΔG_{12} and ΔG_{23} are the free energies of cooperative interaction between adjacent occupied sites, defined as the difference between ΔG_s for any species and the sum of the intrinsic free energies of binding to the occupied sites.

to multiple, specific sites on DNA. However, in order to resolve even macroscopic binding parameters from filter binding data, it is necessary to assume a specific relationship between the number of ligands bound to the DNA and the retention of the protein–DNA complex by the filter. Our results with the λ system show conclusively that no such relationship exists. Consequently, it is impossible by filter binding titration experiments to resolve thermodynamically correct macroscopic binding parameters, and therefore to resolve the microscopic binding and cooperativity constants even with the additional information provided by the mutant operators.

Theory

In this section, we present the binding expressions for the interactions of *cI* repressor with the bacteriophage λ lysogenic/lytic control region. The two operators, O_R and O_L, control transcription of the *cI* gene and of other genes involved in viral replication and host cell lysis (Ptashne & Hopkins, 1968; Eisen et al., 1979). Repressor binds cooperatively to adjacent sites of the operators, a crucial feature of the control mechanism (Ackers et al., 1982; Shea & Ackers, 1985).

A statistical–thermodynamic model for these interactions was presented previously (Ackers et al., 1982). The salient features are represented by the configurations of the operator shown in Table I. The total free energy of each species, relative to the unligated reference species, is given as the sum of contributions of five free energies. The intrinsic free energies of binding to each of the three sites are denoted by ΔG_1, ΔG_2, and ΔG_3. We define the free energy of cooperative interaction between adjacently liganded sites (ΔG_{ij}) as the difference between the free energy to fill the two sites simultaneously and the sum of the free energies required to fill them individually, i.e., the sum of the intrinsic free energies.

Individual Site Binding Expressions. Binding expressions for the individual sites of the λ operators are constructed by considering the relative probability, f_s, of each operator configuration:

$$f_s = \frac{\exp(-\Delta G_s/RT)[R_2]^j}{\sum_s \exp(-\Delta G_s/RT)[R_2]^j} \quad (1)$$

where ΔG_s is the sum of free energy contributions for configuration "s" (Table I), R is the gas constant, T is the absolute temperature, $[R_2]$ is the concentration of free repressor dimer, and j is the number of repressor dimers bound to a given configuration, s. The summation over s in the denominator is taken from 1 to 9 for O_L^+ and from 1 to 8 for O_R^+ (Ackers et al., 1982). The fractional occupancies of the O_L^+ sites are given by

$$\bar{Y}_{O_L1} = f_2 + f_5 + f_6 + f_8 + f_9 \quad (2a)$$

$$\bar{Y}_{O_L2} = f_3 + f_5 + f_7 + f_8 + f_9 \quad (2b)$$

$$\bar{Y}_{O_L3} = f_4 + f_6 + f_7 + f_8 + f_9 \quad (2c)$$

In principle, all five interaction free energies defined in the previous section are resolvable when individual site binding data for the wild-type operator are analyzed according to this system of simultaneous equations.

Binding expressions for mutant operators in which specific binding to one or more sites is eliminated are easily constructed for the configurations in Table I. For example, only configurations 1, 3, 4, and 7 exist for O_R1^-. The binding expressions are

$$\bar{Y}_{O_R1} = 0 \quad (3a)$$

$$\bar{Y}_{O_R2} = f_3 + f_7 \quad (3b)$$

$$\bar{Y}_{O_R3} = f_4 + f_7 \quad (3c)$$

Individual Site Loading Free Energies. Each individual site binding isotherm (for mutant or wild-type operators) provides a measure of the total chemical work to bind a mole of ligand at the respective site, while stoichiometric amounts of ligand are also bound to the other sites. This chemical work is the *individual site loading free energy* ($\Delta G_{l,i}$) of Ackers et al. (1983). The loading free energy includes all contributions that affect binding of ligand at site i, including those generated by binding reactions at neighboring sites. Changes in the macromolecular interactions due to structural perturbations of the macromolecules, or due to changes in environmental conditions, will be reflected in these $\Delta G_{l,i}$ values. The loading free energies can be evaluated directly from the individual site binding data, in a model-independent manner, by numerical integration according to

$$\Delta G_{l,i} = RT \ln [\bar{X}_i] = RT \int_0^1 \ln [X] \, d\bar{Y}_i \quad (4)$$

$[X]$ is the free ligand activity (denoted by $[R_2]$ when the ligand is repressor dimer) and $[\bar{X}_i]$ the median ligand activity defined by Wyman (1964).

Binding Expressions for the Filter Binding Method. Nitrocellulse filters retain DNA molecules that have at least one ligand (protein) bound but do not retain unliganded DNA. The expression that defines this separation (Clore et al., 1982) is

$$\theta = [DNA_{bound}]/[DNA_{total}] = (Z - 1)/Z \quad (5)$$

where Z is the binding polynomial (Wyman, 1964) given by

$$Z = \sum_{i=0}^{n} K_i[L]^i \quad (6)$$

K_i is the macroscopic association constant for the reaction DNA + iL $\rightleftharpoons$ DNA·L$_i$, [L] is the free ligand concentration, and n is the number of binding sites. The binding expression for the three-site λ operators is

$$\theta = \frac{K_1[R_2] + K_2[R_2]^2 + K_3[R_2]^3}{1 + K_1[R_2] + K_2[R_2]^2 + K_3[R_2]^3} \quad (7)$$

Each macroscopic constant in eq 7 reflects the sum of configurations in Table I with i ligands bound. Thus, the relationships between the K_i values and the microscopic equilibrium constants k_1, k_2, k_3, k_{12}, and k_{23} corresponding to the interaction free energies of Table I can be written:

$$K_1 = \frac{[DNA\cdot R_2]}{[DNA][R_2]} = k_1 + k_2 + k_3 \quad (8a)$$

$$K_2 = \frac{[DNA\cdot(R_2)_2]}{[DNA][R_2]^2} = k_1k_2k_{12} + k_1k_3 + k_2k_3k_{23} \quad (8b)$$

$$K_3 = \frac{[DNA\cdot(R_2)_3]}{[DNA][R_2]^3} = k_1k_2k_3(k_{12} + k_{23}) \quad (8c)$$

It is evident that the three macroscopic association constants of eq 7 do not uniquely define the five interaction energies of Table I.

A complication of the filter binding assay is that even tight protein–DNA complexes are retained by the filters with less than 100% efficiency. In the worst cases, the retention efficiency is near zero (Eliason et al., 1985; also see below). The quantity experimentally observed is the fraction (F_R) of DNA retained by the filters. To relate this quantity to the macroscopic constants K_1, K_2, and K_3, it is necessary to include retention effeciency terms for each state of ligation, i.e.

$$F_R = \frac{r_1K_1[R_2] + r_2K_2[R_2]^2 + r_3K_3[R_2]^3}{1 + K_1[R_2] + K_2[R_2]^2 + K_3[R_2]^3} \quad (9)$$

where r_i is the retention efficiency for DNA with i repressors bound. The only r_i uniquely determined by the binding data is r_3, the observed retention at saturation with repressor. It is necessary to relate each of the r_i values to the observed maximum retention if eq 9 is to be used to evaluate the macroscopic constants K_1, K_2, and K_3. Woodbury and von Hippel (1983) have suggested that each liganded site on the DNA exhibits a fixed and independent probability of retention. This leads to

$$r_i = 1 - \zeta^i \quad (10)$$

where ζ is the probability that a liganded site will pass through the filter without being retained. We refer to this as the "independent probability model". Another possibility is that the retention efficiency is constant for any liganded DNA and does not depend on the stoichiometry of the complex. This leads to simple normalization of the data to the maximum retention (all r_i's equal to F_R^{max}). We refer to this as the "constant probability model".

Often, parameters that appear separately in model equations are still correlated, such that, in analyzing experimental data, variations in one are compensated by corresponding variations in one or more of the others [see Turner et al. (1983)]. The macroscopic equilibrium constants (K_i) and the retention factors (r_i) of eq 9 are highly correlated in this sense. Only in the limit of infinite retention efficiency (all r_i = 1) will the same equilibrium constants describe identical curves for the two models. Otherwise, it will generally be necessary for the binding data themselve to distinguish between these mutually exclusive models, if the macroscopic equilibrium constants are to be accurately estimated. A major question to be answered is whether filter binding data are capable of making this distinction.

Materials and Methods

Chemical Reagents. α-^{32}P-Labeled deoxyribonucleotides (3000 Ci/mmol) were purchased from Amersham; unlabeled deoxyribonucleotides were from P-L Biochemicals. Electrophoresis grade acrylamide, bis(acrylamide), ammonium persulfate, and TEMED were supplied by Bio-Rad. Acrylamide and bis(acrylamide) were deionized by using Bio-Rad AG 501-X8 mixed-bed resin prior to use. All other reagents were reagent or analytical grade.

Biological Materials. The large fragment (Klenow) of DNA polymerase I and the restriction enzymes *Bgl*II and *Eco*RI were purchased from New England Biolabs. *Hae*III, *Hin*dIII, and *Pst*I were from Bethesda Research Labs (BRL). Bovine pancrease deoxyribonuclease I (DNase I, code DP) from Worthington was stored as a 2 mg/mL stock solution in 50% glycerol at −70 °C. Transfer RNA (type XX) was from Sigma. Bovine serum albumin (BSA) was from BRL, and calf thymus DNA (CT DNA) was from P-L Biochemicals.

Repressor protein was isolated by using the procedure of Johnson (1980) with some modifications (Brenowitz et al., 1986). The repressor is greater than 95% pure as estimated by electrophoresis on NaDodSO$_4$. From stoichiometry experiments of the type described by Sauer (1979) and by Johnson (1980), we estimate the repressor to be 79% active.[2] Total monomer concentrations were corrected for this activity prior to calculation of the dimer concentration. A dimer to monomer dissociation constant of 2.0×10^{-8} M (Sauer, 1979) was assumed.

Preparation of Radiolabeled DNA Fragments. DNA fragments used in these studies were derived from the following sources. Plasmids pBJ301, pBJ303, pBJ306 (Meyer et al., 1980), and pAH19 (Maurer et al., 1980) containing λ right operator DNA were gifts from J. Eliason and M. Ptashne. The binding competencies are O_R1^-, $O_R1^-3^-$, O_R2^-, and O_R3^-, respectively. These were grown in *Escherichia coli* strain HB101. *E. coli* strain MM294 cells transformed with either pKB252 (O_R^+, Backman et al., 1976) or pO_R1 (Roberts et al., 1979) were gifts from H. Helson and R. Sauer. The latter contains an operator from which sites O_R2 and O_R3 are deleted. The O_L^+-containing plasmid, pKC30 (Shimatake & Rosenberg, 1981), was a gift from M. Wold and R. McMacken.

Plasmids were purified by the procedure of Birnboim and Doly (1979) followed by CsCl density gradient centrifugation (Maniatis et al., 1982) and electrophoresis on 1% agarose gels. The operator-containing fragment (648 bp) was cut from plasmids pBJ301, pBJ303, pBJ306, pAH19, and pKB252 with *Bgl*II and *Hin*dIII. A 570 bp O_R1-containing fragment was cut from pO_R1 with *Eco*RI. A shorter 155 bp fragment was

[2] A preliminary estimate of 46% active was used in the analysis of data in earlier publications (Brenowitz et al., 1986a,b). This was shown to be incorrect by an extensive series of stoichiometry measurements made prior to the analysis of the data presented here. The resulting error in the repressor concentration scale in the earlier publications accounts for the slight differences between the interaction free energies reported here and those reported previously.

produced by cutting again with *Hae*III [see Brenowitz et al. (1986)]. The shorter fragment was used for footprint titration experiments since it is necessary to have only one strand of the DNA labeled. A 248 bp O_R^+-containing fragment was cut from pKC30 by using *Bgl*II and *Hae*III. DNA fragments were isolated by electrophoresis through 1.5% agarose gels and purified by chromatography on DEAE-Sephadex (Maniatis et al., 1982) or on NACS-prepac (BRL) according to the manufacturer's suggested protocol.

Fragments were labeled with α-^{32}P-labeled deoxyribonucleotides at their 3′ recessed ends by using Klenow polymerase (Maniatis et al., 1982). The typical specific radioactivity of the DNA was 9×10^6 Ci/mol. The 648 bp fragments from pBJ301, pBJ303, pJB306, pAH19, and pKB252 were labeled only at their *Bgl*II end. This was accomplished by isolating fragments larger than 648 bp from these plasmids, labeling with α-^{32}P-labeled deoxyribonucleotides as described, and then cutting with *Hin*dIII.

Equilibration of Binding. Reactions were equilibrated in a water bath at 20 ± 0.5 °C for at least 40 min and up to 2 h prior to binding assays. Binding measurements (by either method) did not depend on the incubation time, over this range. All binding experiments were conducted in a buffer (assay buffer) consisting of 10 mM Bistris (pH 7.00 ± 0.01), 2.5 mM $MgCl_2$, 1.0 mM $CaCl_2$, 0.1 mM EDTA, 0.200 M KCl, 100 μg/mL BSA, and 2 μg/mL CT DNA (sonicated).

Nitrocellulose Filter Binding Measurements. Nitrocellulose filters (0.45 μm) obtained from Schleicher & Schuell and from Millipore were used. The Millipore filters gave slightly less background retention in the absence of repressor and 10–20% greater retention at saturation with repressor than did the Schleicher & Schuell filters. However, in no case did the fitted binding parameters or shape of the observed binding curve depend on the manufacturer. Filters were soaked in wash buffer (assay buffer, less BSA and CT DNA) for 1–2 h before use.

Two aliquots from each equilibrated reaction mixture were separately filtered to give replicate measurements. Each filter was washed twice with 0.5 mL of wash buffer. The flow rate for these steps was controlled at approximately 50 mL/h by using a peristaltic pump. Typically, 3000–5000 cpm of DNA was applied to each filter (or less than 4 pM in operator). Under these conditions, the background retention was 1–2% of the total radioactivity applied. The total DNA concentration was determined by counting aliquots of control binding reaction mixtures which were not filtered.

DNase I Footprint Titration Measurements. A complete description of the DNase footprint titration technique is presented elsewhere (Brenowitz et al., 1986). Equilibrium mixtures contained repressor concentrations as indicated and 15 000–20 000 cpm of ^{32}P-labeled operator DNA (or less than 16 pM). This concentration of operator is similar to the dissociation constant for repressor dimer from the tightest binding sites. However, the repressor dimer concentration is effectively buffered by the large excess of monomers with which it is in equilibrium. Therefore, it was unnecessary to correct for the total operator DNA concentration, which is not accurately known.

DNase I exposure was initiated by addition of 75–120 ng of enzyme in 5 μL. Reactions were stopped after 0.5 or 1.0 min by addition of 0.700 mL of 92% (v/v) ethanol, 0.57 M ammonium acetate, and 50 μg/mL tRNA, precooled to −70 °C. The DNA was precipitated for at least 15 min at −70 °C and pelleted in a microfuge. Each pellet was rinsed twice with 1.5 mL of 80% ethanol, dried, and dissolved in 5 μL of 80% (v/v) dionized formamide, 89 mM Tris–borate (pH 8.3), 1 mM EDTA, and tracker dyes.

The samples were electrophoresed at constant power (50–70 W) on 6% polyacrylamide–urea sequencing gels (38 cm × 32 cm × 0.4 mm) as described by Maxam and Gilbert (1980). The DNA was heat denatured at 90 °C for 10 min, rapidly cooled to 0 °C, and immediately loaded on a preelectrophoresed gel. Autoradiography of the dried gels was conducted at −70 °C by using preflashed (Laskey & Mills, 1977) Kodak X-OMAT film and a single Dupont Cronex Lightening Plus intensifying screen.

The optical density of the film was scanned in two dimensions by an Optronix P-1700 rotating drum scanner. The scanner discriminates 256 levels of optical density from 0 to approximately 1.5 ODU. The array of optical densities (corresponding to 200 μM pixels on the gel) was processed interactively by using programs developed in this lab. Protein binding is monitored by the ratio of the total, or integrated, optical density of a series of bands which correspond to a binding site to the optical density of a similar series of bands outside the binding site.

Computing Procedure. The experimental data were analyzed according to the mathematical functions described in the text by using nonlinear least-squares procedures (Johnson et al., 1976; Turner et al., 1983) to estimate the model-dependent parameters, e.g., interaction energies and retention factors, and their 65% confidence intervals. All calculations were performed with an HP-1000 computer system.

RESULTS

Footprint Titration Analysis of Repressor Binding to O_L. Binding of *cI* repressor protein to O_L^+ was studied by using the footprint titration method (Figure 1). Each set of 30 data points relates the fractional saturation of one binding site to the concentration of free repressor dimer with which it is in equilibrium. The steepness of the isotherms for sites O_L1 and O_L2 is indicative of the cooperative nature of the binding. These curves are sigmoidal when plotted on a linear scale.

Unique resolution of all of the interaction energies is not always possible for highly cooperative systems, such as the λ left operator, using binding data for the wild-type operator alone. Some of the parameters in eq 2a–c are highly correlated as a consequence of the coupling between the sites (see Discussion). Due to this complication, the data in Figure 1 were only able to be analyzed subject to the constraint $\Delta G_{12} = \Delta G_{23}$. (We show below how all of the free energies can be obtained for systems like O_L, using reduced valency mutant operators.) Equations 2a–c were solved to give the best estimates for ΔG_1, ΔG_2, and ΔG_3 for various fixed values of ΔG_{12} (and ΔG_{23}).

The results of this analysis, summarized in Figure 2, clearly indicate negative values for the cooperative free energy terms (i.e., positive cooperativity). A lower limit to the magnitude of the cooperative free energies was estimated by comparing the ratios of the variances of the fits (Figure 2) to the *F* statistic for the 65% confidence interval (Turner et al., 1983). The curves plotted in Figure 1 reflect this limit; these are the curves predicted by the fitted parameters with $\Delta G_{12} = \Delta G_{23} = -2.5$ kcal/mol. Notice that while ΔG_2 is highly dependent on ΔG_{12} and ΔG_{23}, ΔG_1 and ΔG_3 are not. These values are well resolved irrespective of the magnitude of the cooperativity. In addition, despite the uncertainty in some of the model-dependent parameters (ΔG_2, ΔG_{12}, and ΔG_{23}), the individual site loading free energies are precisely determined from the observed data points by using eq 4. This yields $\Delta G_{1,1} = -14.3 \pm 0.2$ kcal/mol, $\Delta G_{1,2} = -14.1 \pm 0.2$ kcal/mol, and $\Delta G_3 = -12.9 \pm 0.2$ kcal/mol.

Table II: Macroscopic Free Energies Derived from Filter Binding Titration of Repressor Binding to O_L^+ [a]

	retention model[b]				
	independent probability		constant probability		
parameter	two site	three site	two site	three site	predicted[c]
ΔG_1^M (kcal/mol)	−14.0 ± 0.2	−14.0 ± 0.2	−13.8 ± 0.1	−13.8 ± 0.1	−13.9
ΔG_2^M (kcal/mol)	−28.2 ± 0.2	−28.3 ± 0.3	−28.0 ● 0.3	−28.1 ± 0.2	−28.5
ΔG_3^M (kcal/mol)		−39.5 ± 1.7		>−41	−41.3
ζ[b]	0.44 ± 0.04	0.48 ● 0.06			
F_R^{max}[b]			0.79 ± 0.03	0.80 ± 0.03	
D[d]	0.014	0.013	0.014	0.014	

[a] Free energies (with 65% confidence limits) corresponding to the macroscopic binding parameters, K_1, K_2, and K_3 of eq 9, for the data of Figure 3. Data were fit with and without the terms in K_3 to give the three-site and two-site results, respectively. [b] Retention model refers to the definition of the retention factors, r_i, for complexes with i ligands bound. These definitions are given by $r_i = 1 - \zeta^i$ (eq 10 in text) and $r_i = F_R^{max}$ (the retention at saturation) for the independent probability and constant probability models, respectively. [c] Values predicted from the microscopic interaction free energies (Figure 2, middle solution) estimated for the data of Figure 1. [d] Weighted mean deviation of the fitted curves, given by $D = [\sum_i w_i(\bar{Y}_i - \hat{Y})^2/\sum_i w_i]^{1/2}$. Weights assigned were proportional to $1/F_R^{obsd}$ on the basis of the observation (see Figures 3, 4, and 5) that the error in measuring F_R is proportional to F_R^{obsd}.

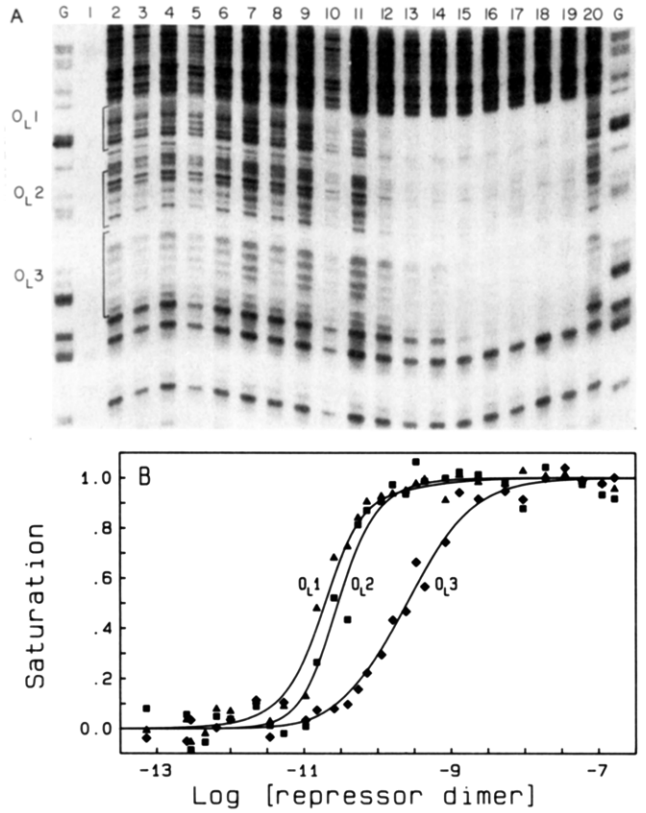

FIGURE 1: Footprint titration of repressor binding to O_L^+. Reaction conditions are in the text (Materials and Methods). (A) Autoradiogram of the DNA after exposure to DNase I, showing increasing protection from hydrolysis in the repressor binding sites with increasing [repressor]. The outside lanes (labeled G) show the guanine-specific cleavage reaction of Maxam and Gilbert (1980) used to outline the binding sites. Lane 1 is a control showing the nicking of the labeled strand prior to exposure to DNase I. Total repressor concentrations, in monomer units, are (lane 2) 0, (lane 3) 38 pM, (lane 4) 57 pM, (lane 5) 77 pM, (lane 6) 0.11 nM, (lane 7) 0.17 nM, (lane 8) 0.27 nM, (lane 9) 0.38 nM, (lane 10) 0.57 nM, (lane 11) 0.96 nM, (lane 12) 1.3 nM, (lane 13) 2.1 nM, (lane 14) 3.3 nM, (lane 15) 5.7 nM, (lane 16) 11 nM, (lane 17) 33 nM, (lane 18) 96 nM, (lane 19) 0.27 μM, and (lane 20) 0. Operator DNA concentration was 5 pM. (B) individual site binding data. Extent of saturation for sites O_L1, O_L2, and O_L3, determined as described in the text from the autoradiogram in panel A and from a companion experiment. (Triangles) O_L1; (squares) O_L2; (diamonds) O_L3. Solid curves drawn through the points are the fitted curves according to eq 2. The estimated interaction free energies (middle solution, Figure 2) are $\Delta G_1 = -13.8 \pm 0.3$ kcal/mol, $\Delta G_2 = -12.1 \pm 0.2$ kcal/mol, $\Delta G_3 = -12.4 \pm 0.2$ kcal/mol, and $\Delta G_{12} = \Delta G_{23} = -2.5$ kcal/mol.

Filter Binding Analysis of Repressor Binding to O_L. Binding of repressor to O_L was also studied by using the nitrocellulose filter binding assay (Figure 3). These data were analyzed according to eq 9, using each retention model in turn, to give the best estimates for K_1, K_2, K_3, and either ζ (independent probability) or F_R^{max} (constant probability). Sites O_L1 and O_L2 are nearly saturated before O_L3 begins to fill (Figure 1). In this case, the constant probability model predicts that

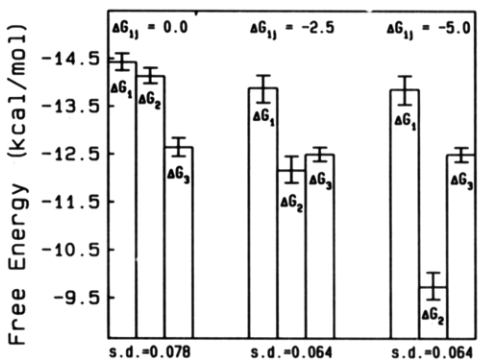

FIGURE 2: Estimated interaction free energies for repressor binding to O_L^+ when the data in Figure 1 were fitted to eq 2. ΔG_{ij} refers to ΔG_{12} and ΔG_{23} of Table I. These were set equal to 0.0, −2.5, or −5.0 kcal/mol; ΔG_1, ΔG_2, ΔG_3, and their 65% confidence limits (represented by error bars) were estimated. s is the square root of the variance of the fitted curves. The estimated interaction energies for $\Delta G_{ij} = -2.5$ kcal/mol predict the solid curves in Figure 1. The isotherms predicted by all three solutions are compared in Figure 7.

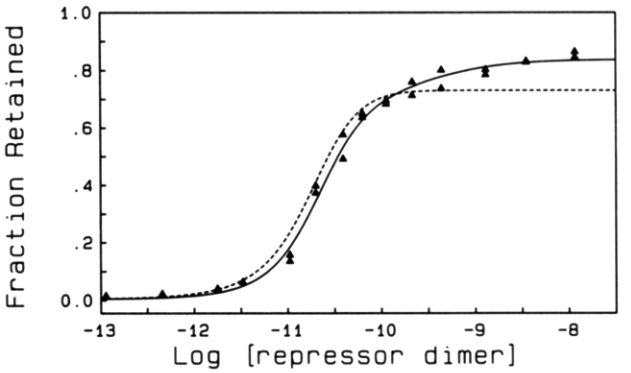

FIGURE 3: Filter binding titration of repressor binding to O_L^+. Replicate measurements of the fraction of operator DNA retained by the filters at each repressor concentration. The data were analyzed according to eq 9, with retention factors (r_i) adhering to either the independent probability or the constant probability of retention models (see text). The free energies corresponding to the resultant macroscopic binding parameters are in Table II. The curves are predictions from the footprint titration data of Figure 1. The solid and dashed lines represent the independent and constant probability of retention models, respectively.

the filter binding data will be insensitive to the presence of the third site. The independent probability model requires the opposite. Therefore, the data were also analyzed according to eq 9, where the last term in both the numerator and the denominator was omitted (i.e., a two-site expression) to test the ability to resolve K_3.

The results of these analyses (Table II) highlight the insensitivity of the filter binding experiment to the number of sites, as predicted by the constant probability model. In fact, K_3 is not justified in either model by improved variance of the fit or by a more random distribution of residuals. In addition, the estimated K_1 and K_2 values are independent of K_3 in both cases. However, despite the fact that this insensitivity to the third site contradicts the independent probability model, the data do not distinguish between these mutually exclusive models. The differences between the fitted parameters for the two models are well within experimental error, though they are systematic.

To further explore the issue of the correct retention model, and the confidence one can place in the estimated K_3, the filter binding data were compared to isotherms predicted by the individual site binding data for O_L^+. The curves in Figure 3 are obtained by using K_1, K_2, and K_3 (of eq 7) calculated according to eq 8, using the microscopic free energies estimated from the data in Figure 1. The free energies corresponding to the values of K_1, K_2, and K_3 so calculated are listed in Table II. It is clear from the curves that the two experiments do not agree if the constant probability model is correct; they are consistent with one another if the independent probability model is correct, but only if the terms in K_3 are included in the comparison. Thus, neither retention model rationalizes all of the experimental observations.

Comparison of Footprint Titration and Filter Binding To Monitor Binding at a Single Site. The apparent paradox would be explained if the retention factors predicted by the independent probability model are similar to, but systematically different from, the actual retention efficiencies of the various ligation states. It could also be the result of systematic errors in one or both experiments. The filter binding assay physically separates liganded DNA from the free ligand with which it is in equilibrium. This separation must be performed rapidly relative to the half-lives of the complex. By contrast, the footprint assay is independent of the length of exposure to DNase I (Brenowitz et al., 1986a,b); the limited exposure to DNase I has no measurable effect on the equilibrium distribution of operator configurations. Thus, the susceptibility of the two experiments to at least one type of experimental artifact is substantially different.

The possibility of experimental artifacts was eliminated by control experiments conducted on the single-site DNA template from pO_R1. The simplicity of a single-site system allows systematic differences between the experiments to be assessed. The fractional saturation (Y_1) and the fraction of liganded DNA (θ) are both given by the familiar Langmuir isotherm

$$\bar{Y}_1 = \theta = \frac{k_1[R_2]}{1 + k_1[R_2]} \qquad (11)$$

Here the retention factor (r_1 of eq 9) is a normalization constant relating F_R to θ. Its interpretation is unambiguous. The isotherms resolved by the two experimental methods (Figure 4) and the experimental precision are the same, attesting to the accuracy of both techniques, and supporting the conclusion that both probe the equilibrium thermodynamics of the system.

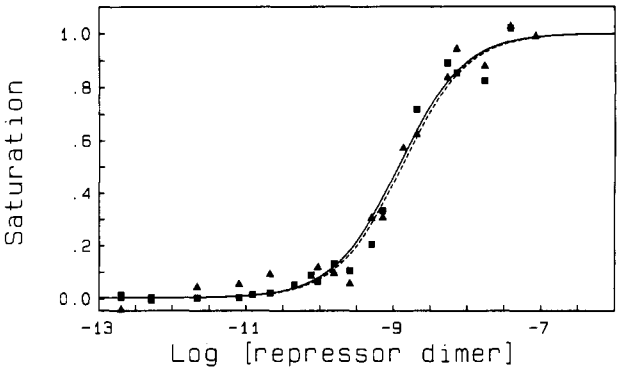

FIGURE 4: Comparison of footprint titration and filter binding titration of repressor binding to O_R1. The triangles are footprint titration measurements. The solid curve is the fit of eq 10, which yields $\Delta G = -12.0 \pm 0.1$ kcal/mol ($s = 0.06$). The squares are the means of replicate filter binding measurements, scaled by the maximum retention (0.10) to give fractional saturation. These yield $\Delta G = -11.9 \pm 0.2$ kcal/mol (dashed curve; $s = 0.05$).

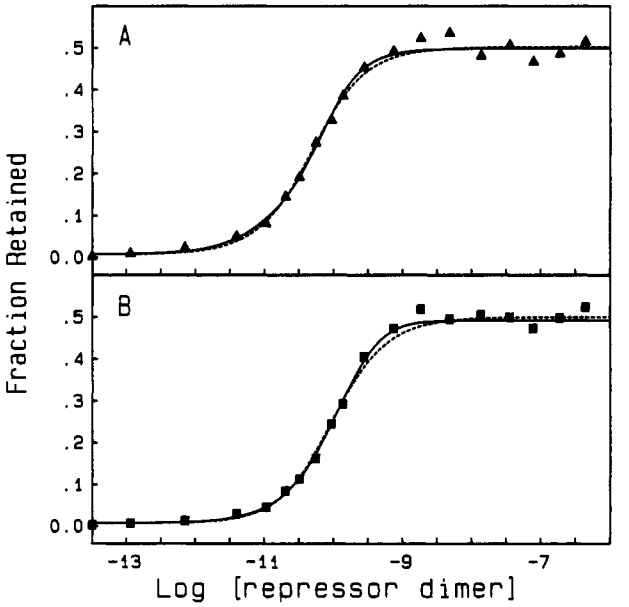

FIGURE 5: Filter binding titration of repressor binding to O_R^+ and O_R3^-. DNA fragments (648 bp) differ by only a single base pair in site O_R3. Points are the means of replicate measurements. The data were analyzed according to eq 9, with retention factors adhering to the independent probability, constant probability, and empirical probability of retention models (see text). The free energies corresponding to the estimated macroscopic binding parameters are in Table IV. (A) Repressor binding to O_R^+. The curves are fitted curves for the independent probability model. The solid curve assumes three repressor binding sites; the dashed curve assumes only two binding sites. (B) Repressor binding to O_R3^-. The curves are fitted curves assuming two repressor binding sites. The solid and dashed curves represent the constant probability and empirical probability models, respectively. The independent probability model yields a curve intermediate between these.

Repressor Binding to O_R^+ and to Reduced Valency Mutant Operators. The question of the relative filter binding retention efficiencies of the intermediate ligation states of multiple-site systems was studied further, by using the λ right operator. We made use of mutants of the right operator in which a single base pair substitution in one or more of the repressor binding sites severely reduces the affinities of the altered sites for repressor (Meyer et al., 1980). When saturated with repressor, each of these reduced valency mutants corresponds to one of the operator configurations of Table I. If a 1 base pair difference in sequence has no direct effect on the retention efficiency, then the maximum retentions for these reduced va-

Table III: Retention by Nitrocellulose Filters of Individual Configurations of O_R[a]

operator	configuration[b]	obsd F_R^{max}	predicted F_R^{max}[c] independent probability	predicted F_R^{max}[c] constant probability
O_R^+	8	0.50 ± 0.01	0.50	0.50
O_R1^-	7	0.13 ± 0.01	0.37	0.50
O_R2^-	6	0.05 ± 0.02	0.37	0.50
O_R3^-	5	0.50 ± 0.01	0.37	0.50
O_R1^-, O_R2^-	4	nd[d]	0.21	0.50
O_R1^-, O_R3^-	3	0.02 ± 0.004	0.21	0.50
O_R2^-, O_R3^-	2	0.10 ± 0.01[e]	0.21	0.50

[a] Values are the asymptotic retentions at saturation with repressor (F_R^{max}) from filter binding experiments conducted on 648 bp DNA fragments containing the indicated operator. The reduced valency mutant operators used differ by only one base pair in each mutated site. All experiments were conducted by using filters supplied by Schleicher & Schuell. [b] Species number of the configuration of the fully saturated operator (Table I). [c] Predicted retention for each configuration, according to the independent and constant probability of retention models, assumes F_R^{max} = 0.50 for O_R^+. [d] Value not determined. [e] Value obtained by using DNA from pO_R1 (see Materials and Methods) of either 155 bp (data in Figure 4) or 523 bp. No O_R2^-, O_R3^- operator, constructed by mutation in sites O_R2 and O_R3, exists.

lency operators constitute empirical measurements of the retention efficiencies for all configurations of O_R.

Filter binding experiments were conducted for O_R^+ and four of the six possible reduced valency operators. Since retention efficiency depends to a small extent on the size of the DNA fragment containing the binding sites, these experiments used identical 648 base pair DNA fragments differing by only the single base pair in each of the mutated sites. Representative results in Figure 5 compare isotherms for O_R^+ and O_R3^- operators. This comparison directly addresses the issue of the sensitivity of the filter binding assay to the weakest (see Table V) of the three binding sites. Within experimental error, these isotherms are identical, supporting conclusions drawn from the analysis of the O_L data.

Maximum retentions observed for each of the configurations of O_R studied are in Table III. All are substantially less than unity, so that differences are easily discernible. For comparison, the distributions of retentions predicted by the independent and constant probability models are also listed. Neither model is consistent with the experimental observations. In particular, O_R^+ and O_R3^- show identical retention efficiencies. The independent probability model requires them to be different by 0.13, a quantity 1 order of magnitude greater than the experimental imprecision of the measurement (Table IV). Contrary to the constant probability model, the retention efficiencies of liganded operators vary by 25-fold.

To test the sensitivity of the experimental data to the retention efficiency coefficients (r_i), the O_R filter binding data were analyzed according to three different retention models. First, the r_i values determined empirically (Table III) were used. We refer to this as the empirical retention model. For simplicity, r_1 and r_2 were approximated by the O_R2^-, O_R3^- and by the O_R3^- values, respectively. The configurations represented by these operators (configurations 2 and 5 of Table I) dominate the populations of singly and doubly liganded species, respectively. Fortuitously, these also have the highest retention probabilities (Table III) and so should account for the majority of the experimental signal. In using the O_R2^-, O_R3^- value, the effect of fragment length was ignored; in control experiments, we find the effect to be negligible, in this case. Second, the data were analyzed according to both the independent and constant probability models.

The results of this analysis are shown in Table IV for the O_R^+ data of Figure 5. The reduced valency operators gave similar results. It is evident that the data are equally well described (according to any of the retention models) whether or not the term for the triply liganded state (eq 9) is included in the analysis. These data, like the O_L data, are insensitive to the presence of the third operator site. In addition, the independent probability and constant probability models fit the data as well as does the empirical probability model. The

Table IV: Macroscopic Free Energies Derived for Various Models of Retention of Protein–DNA Complexes by Nitrocellulose from a Filter Binding Titration of Repressor Binding to O_R^+[a]

parameter	retention model: constant probability, two site	constant probability, three site	independent probability, two site	independent probability, three site	empirical probability, two site	empirical probability, three site	calcd[c]
ΔG_1^M (kcal/mol)	−13.8 ± 0.1	−13.8 ± 0.1	−14.0 ± 0.1	−14.4 ± 0.2	−14.6 ± 0.3	−14.9 ± 0.4	−13.7
ΔG_2^M (kcal/mol)	−26.4 ± 0.4	>−26	−27.5 ± 0.1	−27.7 ± 0.4	−28.3 ± 0.2	−28.4 ± 0.2	−27.6
ΔG_3^M (kcal/mol)		−39.3 ± 1.1		−41.5 ± 0.3		−41.5 ± 0.7	−37.8
D[b]	0.012	0.012	0.013	0.012	0.013	0.012	

[a] Free energies (with 65% confidence intervals) corresponding to the macroscopic binding parameters, K_1, K_2, and K_3 (eq 9), for the data of Figure 5A. Retention model refers to the definition of the retention factors (r_i) for each stage of ligation. These definitions are given by the following: constant probability, $r_i = F_R^{max}$ (maximum observed retention); independent probability, $r_i = 1 - \zeta^i$ (eq 10); empirical probability, $r_1 = 0.1F_R^{max}$, $r_2 = r_3 = 0.5F_R^{max}$ (Table III; see Discussion). Data were fit to eq 9 with and without the terms in K_3 to give the three-site and two-site results, respectively. [b] Weighted mean deviation of the fitted curves. The data were weighted as described in the footnotes to Table II. [c] Calculated from the interaction free energies of Table V (first row).

Table V: Free Energies of Interaction for *cI* Repressor Binding to O_R, Resolved by Footprint Titration of O_R^+ and Reduced Valency Mutant Operators[a]

operators	ΔG_1 (kcal/mol)	ΔG_2 (kcal/mol)	ΔG_3 (kcal/mol)	ΔG_{12} (kcal/mol)	ΔG_{23} (kcal/mol)	s[b]
O_R^+, O_R1^-, O_R3^-	−13.7 ± 0.3	−10.3 ± 1.9	−10.2 ± 0.5	−3.6 ± 1.9	−2.9 ± 2.0	0.082
O_R^+, O_R1^-	−13.6 ± 0.4	−10.2 ± 1.7	−10.2 ± 0.5	−3.6 ± 1.8	−2.9 ± 1.9	0.079
O_R^+, O_R3^-	−13.7 ± 0.4	−10.7 ± 0.3	−10.1 ± 0.5	(−3.6)	(−2.9)	0.078
O_R1^-, O_R3^-	−13.8 ± 0.4	−10.3 ± 0.5	−10.1 ± 0.5	(−3.6)	(−2.9)	0.088
O_R^+	−13.6 ± 0.4	−10.2 ± 0.3	−10.1 ± 0.4	(−3.6)	(−2.9)	0.070
O_R1^-		−9.9 ± 1.0	−10.5 ± 1.0		(−2.9)	0.089
O_R3^-	−13.8 ± 0.4	−10.3 ± 0.4		(−3.6)		0.088

[a] Free energies (with 65% confidence intervals) for the interactions defined in Table I. Data (Figure 6) for one or more of the operators were analyzed according to the appropriate binding expressions formulated on the basis of eq 1 (e.g., eqs 3 for O_R1^-). Values in parentheses were fixed for that analysis. [b] Square root of the variance of the fitted curves.

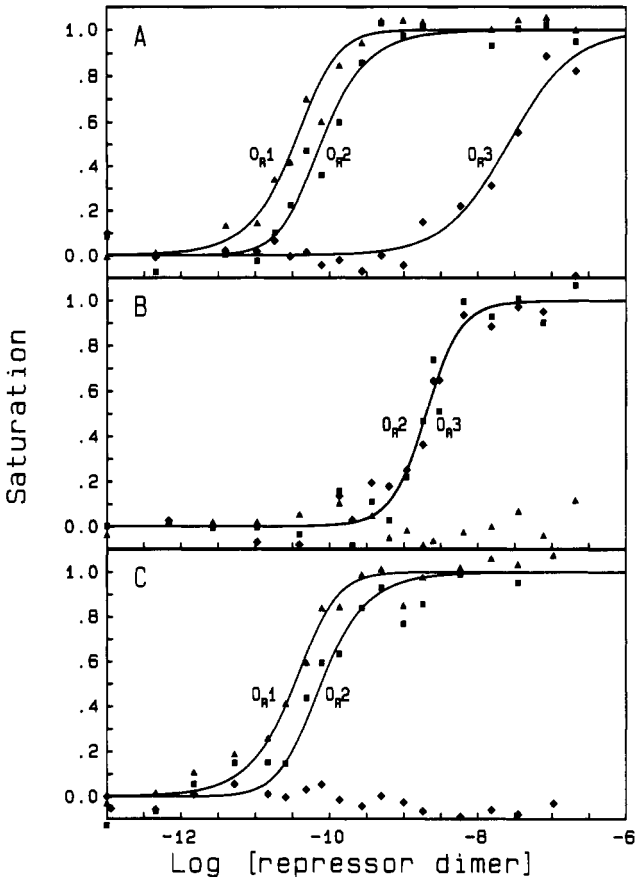

FIGURE 6: Footprint titration of repressor binding to O_R^+ and to reduced valency, mutant operators. DNA fragments used (648 bp) differ by only a single base pair in each mutated site. Panels A, B, and C show O_R^+, O_R1^-, and O_R3^-, respectively. (Triangles) Site O_R1; (squares) site O_R2; (diamonds) site O_R3. The data were analyzed according to the binding expressions (e.g., eq 3) which consider the possible configurations from Table I. The solid curves through the points represent the simultaneous fit to all of the data. Estimated interaction energies are in the first row of Table V.

curves in Figure 5 are representative of the quality of the fits for all of the O_R data and of the differences between the models. Most important, the resolved parameters are highly dependent on the retention model (as expected). The systematic differences between the free energies that are resolved by the various models (e.g., as much as 1.1 kcal/mol for the free energy difference corresponding to K_1) are severalfold larger than the confidence limits. The error that can be introduced by the wrong model is substantial relative to the cooperative free energies for the right operator (Table V).

Individual site binding measurements for O_R^+ and for two reduced valency mutants (O_R1^- and O_R3^-) are shown in Figure 6. The O_R1^- and O_R3^- data indicate that the introduction of a single-point mutation does eliminate binding to the altered site at the concentrations studied. In contrast to the filter binding data, there is no ambiguity as to the number of titratable binding sites. The additional information provided by the reduced valency operator, individual site binding data, does provide a solution to the correlation problem illustrated in Figure 2. The nature of the correlations is changed for the reduced valency operators.

The appropriate systems of simultaneous equations (e.g., eq 3a–c) were solved for various combinations of the wild-type and reduced valency operator data in Figure 6. Results are in Table V. The combined data for all three operators uniquely resolve the values of all five interaction energies. When data for any one operator were considered, the interaction free energies were not all resolved, as expected from Figure 2. For these cases, the cooperative energies (ΔG_{12} and ΔG_{23}) were fixed, equal to the energies resolved from all of the data, and the intrinsic energies (ΔG_1, ΔG_2, and ΔG_3) were estimated. The agreement between all combinations of the operators of all estimated parameters is excellent.

Discussion

The lysogenic to lytic control system of bacteriophage λ is one of many systems in which genome regulation is achieved through the binding of regulatory proteins to multiple, specific DNA sites. In order to relate the relative probabilities of the various configurations of the system to the transcription of genes, it is necessary to develop experimental techniques that are capable of resolving the energetics of each configuration. This study demonstrates that the data produced by the nitrocellulose filter binding assay cannot be unambiguously related to the fractional saturation of the binding sites of a multiple, site-specific system. Even the macroscopic binding parameters are not uniquely resolved. Therefore, these data are useless to deduce the Gibbs energies of the intermediate ligation states. In contrast, the individual site binding data that are resolved by the DNase footprint titration technique separately provide rigorous thermodynamic measurements of the interaction of the protein ligand with every site. These data allow the Gibbs energies to be deduced for each configuration of the binding system.

Use of Filter Binding To Study Site-Specific Binding in Multiple Site Systems. As discussed earlier, the well-known weakness of the filter binding method is that its sensitivity to the binding of additional ligands decreases as the number bound increases (Yarus & Berg, 1970; Hinkle & Chamberlain, 1972; Clore et al., 1982). The problem is acute if the sites are heterogeneous and their number large, or if a single high-affinity site dominates the binding of the first ligand and induces high efficiency of retention by the filters. Since the λ operators contain a small number of sites and are retained with low efficiency, they represent ideal candidates for analysis by this technique.

The formalism presented by Woodbury and von Hippel (1983) represents the only comprehensive treatment of filter binding data that attempts to deal explicitly with the issue of efficiency of retention in such a way that macroscopic binding parameters might be extracted from filter binding measurements on multisite systems. Their treatment is based on the ad hoc assumption that each liganded *site* on the DNA is retained by the filter with a finite, constant probability (less than unity) so that each site behaves independent of the others. As additional ligands are bound, the retention of the DNA will increase to a final asymptotic limit. Only to test the uniqueness of this assumption did we propose the alternative assumption that each liganded DNA *molecule* (regardless of stoichiometry) is retained with a constant probability (less than unity). This predicts no additional retention, after the first ligand is bound.

The fitted parameters (Tables II and IV) indicate that the filter binding data for the interaction of *cI* repressor with either O_L or O_R are well described by either of these mutually exclusive models despite the fact that both are demonstrably wrong. The parameters in Table IV imply, further, that virtually any distribution of the retention factors (r_i) will adequately fit the data and precisely estimate binding constants. The data have no ability to distinguish correct from incorrect models, yet the binding constants that are estimated depend on the model assumed. The availability of reduced valency mutants of O_R provides a unique opportunity to di-

rectly test various retention models. In the absence of the additional information provided by such mutants, the accuracy of the derived constants is impossible to assess, and the filter binding experiment is largely meaningless.

Relationship between Binding Configuration and Filter Retention. The pattern of retention that is observed for the reduced valency operators (Table III) was not caused by the dissociation of ligand from the weakest binding sites (e.g., O_R3) during the assay. If dissociation of repressor from O_R3 had caused the observation that O_R^+ and O_R3^- exhibit equal retention, then the O_R1^- and O_R2^- operators would reflect the retention due to binding at only sites O_R2 and O_R1, respectively. O_R1 binds repressor with greater affinity than O_R2 by several kilocalories per mole (Table V), implying a lower dissociation rate for O_R1 then for O_R2. This predicts that the O_R2^- operator should show greater retention than the O_R1^- operator. It does not. There is only one possible conclusion: each configuration of the operator is indeed characterized by its unique probability of retention.

The consequence of this fact is that there is no simple relation between θ, the fraction of liganded DNA, and F_r, the experimentally observed retention of DNA by the filters, for the case of the λ operators. Each of the constants K_1 and K_2 of eq 9 represents three microscopic configurations of the operator (Table I). Both r_1 and r_2 must be averaged over the three appropriate configurations, each configuration weighted by its fractional population. These fractional populations cannot be calculated unless k_1, k_2, k_3, k_{12}, and k_{23} are known independently. Moreover, the fractional probability as a function of saturation of the operator is different for every configuration. Thus, to rigorously relate θ and F_r requires retention factors (r_i in eq 9) that are themselves complex functions of ligand concentration!

It is unlikely that the binding of the *cI* repressor to the λ operators represents unique examples in the exhibition of configuration-dependent probabilities of retention. Ligand-dependent bending or kinking of DNA at specific sites is by now a well-documented phenomenon [e.g., see Anderson et al. (1981), Frederick et al. (1984), Wu & Crothers (1984) and Dodson et al. (1985)]. A necessary consequence of ligand-induced bending at the site of binding is that the conformation of the the ligand–DNA complex must depend on the configuration as well as on the stoichiometry of bound ligand. Configuration-dependent conformational variation of the protein–DNA complex is a plausible explanation for the variability in retention by a filter that recognizes (binds) only the protein in the complex.

Individual Site Binding Using the Footprint Titration Method. Unlike the filter binding assay, the DNase footprint titration technique does measure fractional saturation, and of the individual sites (Brenowitz et al., 1986a,b). This provides a thermodynamically rigorous method which, unlike any other binding method, is able to discern that repressor binds cooperatively to both operators, on the basis of binding data from the wild-type operators alone. However, there is the complication that three of the five interaction constants that define the free energy states are not uniquely resolved by individual site binding data for the wild-type operator alone. This is not the result of the failure in the experimental technique to provide the necessary precision. Rather the degree of correlation between the parameters of eq 2a–c is a consequence of the free energy coupling between the sites in these cooperatively interacting systems.

Asymptotic Limits to the Shapes of Individual Site Binding Curves. To illustrate this point, consider the individual site

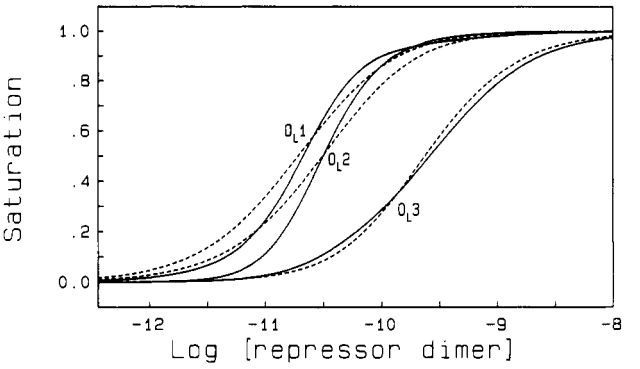

FIGURE 7: Individual site binding curves of repressor binding to O_L^+. Curves are the fits of eq 2 to the data of Figure 1. Estimated interaction energies are represented graphically in Figure 2. The solid and dashed curves represent the theoretical limits of high cooperativity ($\Delta G_{ij} \leq -2.5$ kcal/mol) and of noncooperativity ($\Delta G_{ij} = 0$ kcal/mol), respectively.

isotherms in Figure 7. Each set of isotherms corresponds to one of the three sets of estimated parameters (Figure 2) fit to the O_L^+ binding data in Figure 1. As the cooperativity terms increase in magnitude, the fitted curves approach limiting shapes asymptotically. In fact, for any value of ΔG_{12} (and ΔG_{23}) set less than or equal to −2.5 kcal/mol, the fitted parameters predict the same isotherms (solid curves, Figure 7). At the asymptotic limit, ΔG_2, ΔG_{12}, and ΔG_{23} are infinitely correlated. The startling observation is that the limit is approached at such moderate values of ΔG_{12} and ΔG_{23} at these experimental conditions. This behavior is general for systems of cooperatively interacting sites, but the magnitude of the cooperativity necessary to approach the limit depends on the number of interacting sites, the pattern of cooperative interactions, and the local site binding energies. For the λ operators, we find by simulation of experimental data that as the site heterogeneity increases, the cooperativity necessary to reach the high cooperativity limit also increases. In addition, the difference between the limiting noncooperative and cooperative isotherms (e.g., the dashed and solid curves in Figure 7) is dictated by the pattern of pairwise coupling between the sites. For the λ operators, this difference is small, and the curve shapes are nowhere excessively sensitive to the cooperativity. There is no reason to believe that this is the case for all gene regulatory systems.

Individual Site Loading Free Energies. There is great utility in making individual site binding measurements for regulatory systems for which it may not be possible to resolve all of the microscopic interaction constants from wild-type binding data alone. Important and unique information is still embodied in the individual site isotherms in the form of the individual site loading energies (eq 4). By monitoring $\Delta G_{l,i}$ as a function of environmental conditions such as temperature, pH, and salt concentration, the basis for the macromolecular interactions involved in the regulation may be deduced and the potential for linked equilibrium effects of small molecules assessed. This is particularly crucial for systems, like O_L^+, for which it is not possible to uniquely determine all of the model-dependent interaction constants, but the $\Delta G_{l,i}$ values are precisely determined.

For O_R, where the mutant operators do allow for unique resolution of all of the interaction constants (Table V), the $\Delta G_{l,i}$ values are still of enormous value for two reasons. First, they constrain the values of the model-dependent parameters. The sum of the individual site loading free energies is the total free energy (ΔG_T) to saturate the system. This same ΔG_T must be reflected in the product of interaction constants for the fully

Table VI: Binding Expressions[a] To Describe Repressor Binding to O_R^+ and O_R1^- for the Gel Retardation Binding Technique[b]

(A) O_R^+

$$\theta_0 = 1/(1 + K_1[R_2] + K_2[R_2]^2 + K_3[R_2]^3)$$
$$\theta_1 = K_1[R_2]/(1 + K_1[R_2] + K_2[R_2]^2 + K_3[R_2]^3) \qquad K_1 = k_1 + k_2 + k_3$$
$$\theta_2 = K_2[R_2]^2/(1 + K_1[R_2] + K_2[R_2]^2 + K_3[R_2]^3) \qquad K_2 = k_1k_2k_{12} + k_1k_3 + k_2k_3k_{23}$$
$$\theta_3 = K_3[R_2]^3/(1 + K_1[R_2] + K_2[R_2]^2 + K_3[R_2]^3) \qquad K_3 = k_1k_2k_3k_{12}$$

(B) O_R1^-

$$\theta_0' = 1/(1 + K_1'[R_2] + K_2'[R_2]^2)$$
$$\theta_1' = K_1'[R_2]/(1 + K_1'[R_2] + K_2'[R_2]^2) \qquad K_1' = k_2 + k_3$$
$$\theta_2' = K_2'[R_2]^2/(1 + K_1'[R_2] + K_2'[R_2]^2) \qquad K_2' = k_2k_3k_{23}$$

[a] Expressions for θ_i, the fraction of operators with exactly i ligands bound. K_i and K_i' are macrosopic constants for binding of i ligands to O_R^+ and O_R1^-, respectively. The k_i values are microscopic equilibrium constants corresponding to the free energy contributions described in Table I. [b] Technique of Garner and Revzin (1981) and Fried and Crothers (1981).

ligated configuration(s); e.g., $\Delta G_T = -RT \ln [k_1k_2k_3(k_{12} + k_{23})]$ for species 1–9 in Table I. When compared in this way, the microscopic interaction constants corresponding to the free energies determined for the binding of repressor to O_L^+ (Figure 2) agree exactly with the sum of the $\Delta G_{1,i}$ (text) determined for the same data.

Second, the $\Delta G_{1,i}$ values are useful for first deducing the pattern of free energy coupling that constitutes the correct model. For sites that do not interact cooperatively, $\Delta G_{1,i}$ is simply the local site binding energy. However, if the sites interact cooperatively, each $\Delta G_{1,i}$ must reflect contributions from the coupled sites. For example, when O_R1 is mutated, the free energy released upon saturation of O_R2 decreases by about 1.8 kcal/mol, reflecting the loss of cooperative coupling between O_R1 and O_R2; the free energy released on saturation of O_R3 increases by about 1.5 kcal/mol. These effects are easily seen by comparing the positions of the isotherms for O_R2 and O_R3 in the O_R1^- and O_R^+ operators (Figure 6). Recall that $\Delta G_{1,i}$ reflects the median ligand activity ($\bar{X}_i$, eq 4). By contrast, when O_R3 is mutated, there are only small changes in the other sites. These facts alone indicate (1) that there is cooperative coupling both between O_R1 and O_R2 and between O_R2 and O_R3 in O_R^+ but (2) that the O_R1, O_R2 coupling dominates the cooperativity in O_R^+. Any proposed model must account for these conclusions. No classical binding measurements can provide this crucial information.

Resolution of the Microscopic Parameters. The model proposed in Table I does account for the pattern of coupling inferred from consideration of the individual site loading energies. When individual site binding data from mutant right operators in which one or more sites do not bind repressor appreciably are combined with individual site binding data for O_R^+, all five microscopic free energies are precisely determined (Table V). Ackers et al. (1982) previously used this approach to resolve the energetics of repressor binding to O_R under different experimental conditions. The data were estimates of the repressor concentrations to half-saturate each of the sites ($\bar{Y}_i = 0.5$) for O_R^+ and for five reduced valency mutants. The complete individual site isotherms that are represented by the data in Figure 6 show a similar ability to estimate the energetics and assess the confidence limits for the parameters, using data for O_R^+ and as few as one reduced valency mutant (O_R1^-).

The ability of the individual site binding data to resolve the microscopic interaction constants, using a small number of the possible reduced valency mutant operators, is crucial to the interpretation of the results of the simultaneous analysis of mutant and wild-type data. The binding expressions for the reduced valency mutants (e.g., eq 3a–c) implicitly assume that the interactions at the remaining sites are quantitatively unaffected by single base-pair substitutions in the mutated site(s). The internal consistency of the individual site binding data as indicated by the excellent agreement of the parameters for all combinations of the operators in Table V supports this assumption. In particular, we note that those parameters that are well determined irrespective of the magnitude of the cooperative free energies (e.g., ΔG_1 for O_R^+ and O_R3^- operators) are in good agreement.

For O_R, our simulations of individual site binding data indicate that there are three nonintersecting subsets of the reduced valency operators for which complete individual site binding isotherms, taken together with those for O_R^+, should resolve the five interaction constants. The existence of these independent paths confers an enormous advantage to the footprint titration technique over other methods, both in the assessment of the validity of the assumption regarding the reduced valency mutants and in the ability to critically test molecular models for the cooperativity.[3]

Application of the Mutant Strategy Using Other Binding Techniques. Recent advances in the field of DNA synthesis (Caruthers, 1985) and site-directed mutagenesis [e.g., see Shortle & Botstein (1983) and Zoller & Smith (1983)] greatly facilitate site-specific DNA modification. This makes the reduced valency mutant approach generally attractive. In principle, any binding technique that resolves macroscopic binding parameters for multisite systems provides sufficient information to determine microscopic binding constants using this approach. We assume that the nitrocellulose filter binding assay is unique in its inability to resolve even the macroscopic parameters for multisite systems. In Table VI, we consider the binding expressions appropriate to the right operator, which describe the experimental measurements made by the gel retardation assay (Garner & Revzin, 1981; Fried & Crothers, 1981). This technique measures separately each fraction of molecules (DNA) with exactly i ligands bound (θ_i, $i = 0$ to n for n sites) but without regard to the site of ligation. Notice that the microscopic interaction constants appear only in certain combinations, so that the wild-type isotherms only resolve three composite, macroscopic parameters. However, the binding expressions for the O_R1^- operator define two additional parameters. In principle, this is sufficient to resolve the five microscopic constants.

To compare the gel retardation and footprint titration methods, θ_i (Table VI) and $\bar{Y}_i$ (e.g., eq 3a–c) were calculated for O_R^+ and O_R1^- operators over a range of repressor concentrations. Experimental data were simulated by including random errors in the calculated values. The interaction en-

[3] The assumption that single-pair substitutions in the mutated sites leave the interactions at the remaining sites quantitatively unaltered can be adequately tested only by extensive analysis of individual site binding data for O_R^+ and representatives of all six reduced valency operators (in preparation). Agreement between the parameters estimated by each of the independent paths is a sufficient criterion to accept the validity of the assumption.

ergies were varied to simulate various reaction conditions. In all comparisons, when data of comparable precision were analyzed according to the appropriate expression for θ_i or $\bar{Y}_i$, the two techniques exhibited similar ability to resolve the correct interaction free energies. In contrast, from simulations of the overall fractional saturation of the operator (i.e., $\bar{Y}_T$, the quantity determined by most methods to monitor binding), we found that data for O_R^+ and any small subset of the reduced valency mutants were insufficient to resolve the correct interaction energies.

There are serious limitations to the gel electrophoresis technique. First, the technique relies on maintaining the equilibrium distribution of species during the electrophoretic separation. It has never been demonstrated that this condition is met. Second, the range of experimental conditions is limited since the binding buffer must also be an electrophoresis buffer. Third, for systems like O_R and O_L, no indication of cooperativity is provided from data for any single operator, and the individual site loading energies are not determinable. Nevertheless, the results of our comparisons are encouraging; we hope to stimulate further development of the gel electrophoresis method.

ACKNOWLEDGMENTS

We are grateful to Benjamin Turner for advice and assistance throughout the project.

Registry No. DNase I, 9003-98-9.

REFERENCES

Ackers, G. K., Johnson, A. D., & Shea, M. A. (1982) *Proc. Natl. Acad. Sci. U.S.A. 79*, 1129–1133.

Ackers, G. K., Shea, M. A., & Smith, F. R. (1983) *J. Mol. Biol. 170*, 223–242.

Anderson, J. E., Ptashne, M., & Harrison, S. C. (1985) *Nature (London) 316*, 596–601.

Anderson, W. F., Ohlendorf, D. H., Takeda, Y., & Matthews, B. W. (1981) *Nature (London) 290*, 754–758.

Backman, K., Ptashne, M., & Gilbert, W. (1976) *Proc. Natl. Acad. Sci. U.S.A. 73*, 4174–4178.

Birnboim, H., & Doly, J. (1979) *Nucleic Acids Res. 7*, 1513–1523.

Brenowitz, M., Senear, D. F., Shea, M. A., & Ackers, G. K. (1986a) *Methods Enzymol. 130*, 132–181.

Brenowitz, M., Senear, D. F., Shea, M. A., & Ackers, G. K. (1986b) *Proc. Natl. Acad. Sci. U.S.A.* (in press).

Caruthers, M. H. (1985) *Science (Washington, D.C.) 230*, 281–285.

Clore, G. M., Gronenborn, A. M., & Davies, R. W. (1982) *J. Mol. Biol. 155*, 447–466.

Dodson, M., Roberts, J., McMacken, R., & Echols, H. (1985) *Proc. Natl. Acad. Sci. U.S.A. 82*, 4678–4682.

Draper, D. E., & Gold, L. (1980) *Biochemistry 19*, 1774–1781.

Eisen, H., Brachet, P., Pereira da Saliva, L., & Jacob, F. (1970) *Proc. Natl. Acad. Sci. U.S.A. 66*, 855–862.

Eliason, J. L., Weiss, M. A., & Ptashne, M. (1985) *Proc. Natl. Acad. Sci. U.S.A. 82*, 2339–2342.

Frankel, A. D., Ackers, G. K., & Smith, H. O. (1985) *Biochemistry 24*, 3049–3054.

Frederick, C. A., Grable, J., Melia, M., Samudzi, C., Jen-Jacobson, L., Wang, B., Greene, P., Boyer, H. W., & Rosenberg, J. M. (1984) *Nature (London) 309*, 327–331.

Fried, M., & Crothers, D. M. (1981) *Nucleic Acids Res. 9*, 6505–6525.

Galas, D. J., & Schmitz, A. (1978) *Nucleic Acids Res. 5*, 3157–3170.

Garner, M. M., & Revzin, A. (1981) *Nuclic Acids Res. 9*, 3047–3060.

Hinkle, D. C., & Chamberlin, M. J. (1972) *J. Mol. Biol. 70*, 157–185.

Johnson, A. (1980) Ph.D. Dissertation, Harvard University, Cambridge, MA.

Johnson, A. D., Meyer, B. J., & Ptashne, M. (1979) *Proc. Natl. Acad. Sci. U.S.A. 76*, 5061–5065.

Johnson, M., Halvorson, H., & Ackers, G. K. (1976) *Biochemistry 15*, 5363–5367.

Laskey, R., & Mills, D. A. (1977) *FEBS Lett. 82*, 314.

Maniatis, T., Fritsch, E. F., & Sambrook, J. (1982) *Molecular Cloning—A Laboratory Manual*, Cold Spring Harbor Laboratory, Cold Spring Harbor, NY.

Maurer, R., Meyer, B. J., & Ptashne, M. (1980) *J. Mol. Biol. 139*, 147–161.

Maxam, A. M., & Gilbert, W. (1980) *Methods Enzymol. 65*, 499–540.

Meyer, B. J., Maurer, R., & Ptashne, M. (1980) *J. Mol. Biol. 139*, 163–194.

Ptashne, M., & Hopkins, N. (1968) *Proc. Natl. Acad. Sci. U.S.A. 60*, 1282–1287.

Riggs, A. D., Bourgeois, S., Newby, R. F., & Cohn, M. (1968) *J. Mol. Biol. 34*, 365–368.

Riggs, A., Suzuki, H., & Bourgeois, S. (1970) *J. Mol. Biol. 48*, 67–83.

Roberts, J. M., Kaeich, R., & Ptashne, M. (1979) *Proc. Natl. Acad. Sci. U.S.A. 76*, 760–764.

Sauer, R. (1970) Ph.D. Dissertation, Harvard University, Cambridge, MA.

Schmitz, A., & Galas, D. J. (1983) in *Methods of DNA and RNA Sequencing* (Weisman, S., Ed.) pp 305–347, Praeger, New York.

Shimatake, H., & Rosenberg, M. (1981) *Nature (London) 292*, 126–132.

Shortle, D., & Botstein, D. (1983) *Methods Enzymol. 100*, 457–468.

Turner, B., Pettigrew, D., & Ackers, G. K. (1983) *Methods Enzymol. 76*, 596–628.

Woodbury, C. P., Jr., & von Hippel, P. H. (1983) *Biochemistry 22*, 4430–4437.

Wu, H., & Crothers, D. M. (1984) *Nature (London) 308*, 509–513.

Wyman, J., Jr. (1964) *Adv. Protein Chem. 19*, 224–394.

Yarus, M., & Berg, P. (1970) *Anal. Biochem. 35*, 450–465.

Zoller, M. J., & Smith, M. (1983) *Methods Enzymol. 100*, 468–500.